Environmental Science & Technology

Article

pubs.acs.org/est

On-Road Ammonia Emissions Characterized by Mobile, Open-Path Measurements

Kang Sun,[†,‡] Lei Tao,[†,‡] David J. Miller,[†,‡] M. Amir Khan,[†,‡,§] and Mark A. Zondlo*[,†,‡]

[†]Department of Civil and Environmental Engineering, Princeton University, Princeton, New Jersey 08544, United States

[‡]Center for Mid-Infrared Technologies for Health and the Environment, NSF-ERC, Princeton, New Jersey 08544, United States

Supporting Information

ABSTRACT: Ammonia (NH_3) is a key precursor species to atmospheric fine particulate matter with strong implications for regional air quality and global climate change. NH_3 from vehicles accounts for a significant fraction of total emissions of NH_3 in urban areas. A mobile platform is developed to measure NH_3, CO, and CO_2 from the top of a passenger car. The mobile platform conducted 87 h of on-road measurements, covering 4500 km in New Jersey and California. The average on-road emission factor (EF) in CA is 0.49 ± 0.06 g NH_3 per kg fuel and agrees with previous studies in CA (0.3−0.8 g/kg). The mean on-road NH_3:CO emission ratio is 0.029 ± 0.005, and there is no systematic difference between NJ and CA. On-road NH_3 EFs increase with road gradient by an enhancement of 53 mg/kg fuel per percentage of gradient. On-road NH_3 EFs show higher values in both stop-and-go driving conditions and freeway speeds with a minimum near 70 km/h. Consistent with prior studies, the on-road emission ratios suggest a highly skewed distribution of NH_3 emitters. Comparisons with existing NJ and CA on-road emission inventories indicate that there may be an underestimation of on-road NH_3 emissions in both NJ and CA. We demonstrate that mobile, open-path measurements provide a unique tool to help quantitatively understand the on-road NH_3 emissions in urban and suburban settings.

INTRODUCTION

Ammonia (NH_3) is a key component of the global nitrogen cycle. As the dominant alkaline atmospheric species, NH_3 reacts readily with atmospheric acidic species to form fine particulate matter ($PM_{2.5}$), which has implications for regional air quality and global climate change.[1,2] However, the global sources of NH_3 are subject to considerable uncertainties.[3] The magnitude and trends of emissions from different source types and source regions are even more uncertain. Comparisons between atmospheric modeling and satellite observations imply that current NH_3 inventories are underestimated globally.[4,5] Agricultural cropland/soil and livestock farming are the major sources of atmospheric NH_3 and account for over 60% of the global inventory.[6,7] NH_3 is also a byproduct of fossil fuel combustion, especially from vehicles equipped with three-way catalytic converters (TWC).[8] Existing atmospheric measurements suggest that traffic may provide significant amounts of NH_3 in urban areas,[8−11] although, on a global scale, on-road traffic emissions of NH_3 are considerably smaller compared to agricultural activities. On-road NH_3 emissions may cause greater impact on air quality and human health, because significant sources of other $PM_{2.5}$ precursors (SO_2, NO_x) are usually collocated in heavily populated urban areas.[12] The US EPA monitors ambient NH_3 concentrations in the Passive Ammonia Monitoring Network (AMoN), but NH_3 has not been regulated or controlled from vehicle emissions.[13]

Vehicular NH_3 emissions have been characterized by chassis dynamometer testing,[8,13−18] roadside remote sensing,[19−22] and tunnel measurements.[23,24] Carbon monoxide (CO) and carbon dioxide (CO_2) were usually measured simultaneously to calculate NH_3 emission factors (EFs) and quantify NH_3 emissions. NH_3 EFs are defined as grams of NH_3 emitted per kilogram of fuel burned. NH_3 is especially difficult to measure due to its strong affinity to the instrument surfaces. Its rapid partitioning between gas and particle phase also complicates instrument design.[25] Despite that NH_3 was recognized in vehicle emissions in the 1980s,[26] it is still challenging to represent its real-world emission patterns. Chassis dynamometers can test only a limited range of driving conditions and number of vehicles, whereas on-road NH_3 EF measurements showed substantially skewed distributions, large variances, and time dependence.[20,22] Hence chassis dynamometer tests are not likely representative of the emission patterns of entire vehicle fleets.[27] Roadside remote sensing and tunnel measurements are stationary, which capture representative fleet averages, but they can only characterize emission patterns at a limited number of sites. Furthermore, these sites are often located in tunnels with

Received: October 28, 2013
Revised: January 21, 2014
Accepted: February 11, 2014

dx.doi.org/10.1021/es4047704 | Environ. Sci. Technol. XXXX, XXX, XXX−XXX

significant road gradients (e.g., Caldecott tunnel with a 4% upgrade[24,28]) or on freeway ramps where vehicles drive at low speed, high acceleration, and usually in the presence of a road gradient.[19] The EFs of NH_3, CO, and NO_x have all been shown to have significant positive correlations with vehicle specific power and/or positive road gradients.[17,29−31] Therefore, there are additional challenges to identify roadside measurement sites representative of the route average emissions.[31] Otherwise, EFs are likely biased as uphill driving and high acceleration contribute to high EFs.[17,28,30]

Mobile platforms equipped with fast-response sensors have been previously deployed to quantify on-road emissions.[28,32,33] Mobile on-road measurements can capture emissions under a full range of real-world driving conditions and road conditions. They can also achieve large spatial coverage and measure the average emissions of the entire fleet. Nevertheless, there have been few on-road mobile NH_3 measurements and knowledge about real-world NH_3 EFs is limited. Compared to existing state-of-the-art NH_3 sensors, mobile, open-path sensors are advantageous to quantify on-road emissions. Open-path design shows higher time resolution and faster response.[34−37] It avoids significant adsorption/desorption effects between NH_3 and the instrument surfaces. The delay of response caused by these surface effects may bias the results when NH_3 emission ratios are calculated with other nonsticky tracers, like CO and CO_2. Meanwhile, there is no need to use a powerful pump, which makes the open-path sensors much more portable and adaptable for frequent, long-time on-road measurements.

In this study, we perform measurements with a mobile platform consisting of an open-path NH_3 sensor, an open-path CO sensor, and an open-path CO_2 sensor, all of which are mounted on the top of a passenger car. CO is widely used as a tracer for combustion processes, and the sum of CO and CO_2 provides quantification of vehicle fuel consumption. The high time resolution ($\geq$1 Hz) and fast response of the open-path sensors are especially advantageous for capturing transient concentration changes. The collocation of open-path sensors makes it straightforward to calculate real-time emission ratios. We present both roadside measurements and a series of on-road measurements in a wide range of driving conditions. Our scientific goal is to quantify on-road NH_3 emissions in urban and suburban settings to understand how driving conditions influence on-road NH_3 emissions by making both roadside measurements and a series of on-road measurements under a wide range of driving conditions.

EXPERIMENTAL METHODS

The mobile platform was designed as a 91 × 30 cm breadboard mounted on the base of a car rack, which readily fits on top of most passenger cars. The open-path NH_3 and CO sensors have been described in detail previously in Miller et al.[38] and Tao et al.[37] Only a brief summary is presented here.

Two continuous wave (CW) thermoelectric-cooled distributed feedback (DFB) quantum cascade lasers (QCLs) are used to detect NH_3 and CO at 9.062 and 4.538 μm, respectively. The NH_3 absorption feature at 9.062 μm was selected to optimize the sensitivity while minimizing the interferences from the other species in open-path detection. These two lasers are coupled into multipass optical cells with path lengths of 36 and 16 m, respectively. Wavelength modulation spectroscopy (WMS) is used to enhance the signal-to-noise ratio. The second harmonic (2f) detection in WMS also helps resolve air-broadened absorption lines.[38−40] Detector waveforms are acquired at 50 Hz and coaveraged at 10 Hz. A built-in virtual lock-in amplifier retrieves NH_3 and CO concentrations from the averaged waveforms. Calibration is performed by normalizing an inline ethylene (C_2H_4) reference cell signal in the NH_3 system and an inline acetylene (C_2H_2) reference cell signal in the CO system. The purpose of the inline reference cells is to provide a constant signal that is continuously probed and can be used to account for sensor drift.[40] The accuracies are 10% for NH_3 and 5% for CO, calibrated in situ by the inline reference cells as well as direct absorption spectroscopy. The NH_3 sensor was not calibrated by direction absorption spectroscopy in NJ, which limits the accuracy to 20%.[40] The NH_3 precision is 0.15 ppbv,[38] and the CO precision is 0.36 ppbv[37] at 10 Hz.

A commercial CO_2 sensor, LICOR LI-7500 open-path CO_2/H_2O analyzer, was placed on the mobile platform. The CO_2 sampling frequency was set to 5 Hz with an accuracy <1% and a precision of 0.08 ppmv CO_2. The CO_2/H_2O analyzer was mounted next to the multipass cells of the NH_3 and CO sensors, so the sampling volumes of the sensors have a footprint of 50 × 50 cm. Meteorological parameters were measured by a portable weather station (Vaisala WXT520). Geolocation, car speed, and driving direction were recorded by a GPS unit (GlobalSat EM-406a). All the measurements were averaged at 1 Hz and synchronized with the GPS time stamp. The covariance plots show that NH_3 and CO_2 measurements are synchronized to within 1 s and have similar time response (Supporting Information, Figure S1). Road conditions were recorded by two GoPro Hero3 cameras mounted on the front and back side of the platform. A picture of the mobile platform is shown in the TOC art. All sensors operate on two 12 V car batteries. Emissions from our own vehicle were periodically checked by driving to a relatively clean area with no other traffic emissions. A detailed description of our identification of self-emissions from the measurement vehicles is provided in the Supporting Information (Figure S2).

To derive the emission ratios and EFs from vehicles, we separate the measurements into a slowly varying background and rapidly changing peaks due to individual vehicles. Following the method described by Hudda et al.,[28] we use the lowest percentiles of pollutant concentrations observed during a certain time window as baseline values. A trend line is linearly interpolated between these baseline values. Subtracting the trend lines from the concentration measurements yields the emission enhancement data: $\Delta[NH_3]$, $\Delta[CO]$, and $\Delta[CO_2]$. Sensitivity studies were conducted by calculating emission ratios using a range of time window size (1−30 min). The results show that emission ratio calculation converges within ±5% for time window size of 5−15 min, which indicates that these window sizes are sufficient to separate short time scale vehicle emissions from the long-term regional background. We use a time window of 12 min for consistency. Given that the atmospheric lifetime of NH_3 is about 11 h,[41] and that we are close to the emission sources, we neglect the deposition and phase changes of NH_3 and define NH_3:CO and NH_3:CO_2 emission ratios as $\Delta[NH_3]/\Delta[CO]$ and $\Delta[NH_3]/\Delta[CO_2]$. Empirical cutoffs were selected to exclude data close to the background levels, and thereby to avoid negative and spuriously large values.[42] The ratio calculation is limited to ΔCO greater than 100 ppbv and $\Delta[CO_2]$ greater than 15 ppmv. The emission ratio distributions are insensitive to the cutoffs, and the mean changes within 5% when doubling the cutoffs.

dx.doi.org/10.1021/es4047704 | Environ. Sci. Technol. XXXX, XXX, XXX−XXX

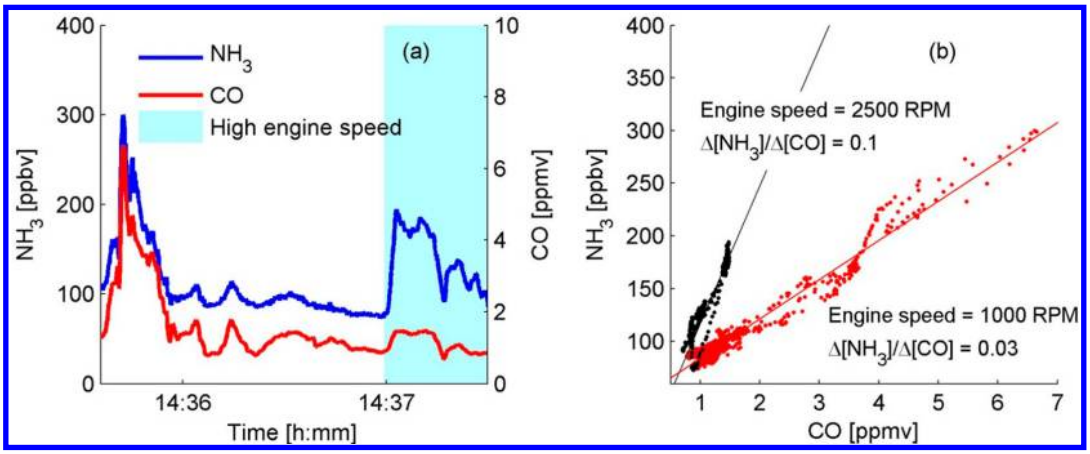

Figure 1. (a) Continuous 10 Hz NH_3 and CO measurements near car exhaust. High engine speed (2500 rpm) period is highlighted. (b) Tracer–tracer plot shows distinct emission ratios at different engine speeds.

RESULTS AND DISCUSSION

Controlled Roadside Measurements. To demonstrate that our sensors could capture the rapid change of concentration and emission ratio with high resolution and sensitivity from individual cars, we deployed the mobile platform in a controlled environment on January 5, 2012. Only NH_3 and CO were measured. The sensors were located inside a parking garage and about 5 m from the exit. The driving speed near the sensor was 7–15 km/h and the vehicles were generally 2–5 m away from the sensor when passing by. The vehicles in the garage were mostly driven by commuters. There were no other significant local sources of NH_3 and CO besides vehicle emissions on campus. We first conducted a static measurement with a 2002 Honda Accord, which uses a three-way catalytic converter. For this test, there were no other vehicles entering or exiting the garage, and the CO concentration was close to the regional background value of 300 ppbv. Figure 1a shows measurements of NH_3 and CO from the car parked 3 m away from the sensor. The variations of NH_3 and CO trace well with each other, and no delay was observed at high time resolution (10 Hz). Initially, the engine was running at an idle speed of 1000 rpm. The measured concentrations varied due to eddy diffusion but the NH_3:CO emission ratio was almost constant ($\Delta[NH_3]/\Delta[CO]$ = 0.03 ppbv/ppbv). Fuel-rich driving conditions were simulated by increasing the engine speed to 2500 rpm, a typical RPM during modest acceleration. As shown by Figure 1b, the NH_3:CO ratio increased significantly when the engine ran fuel-rich, with $\Delta[NH_3]/\Delta[CO]$ = 0.1 ppbv/ppbv. Although this individual car measurement does not represent the engine load in the real world, the result is qualitatively consistent with the literature. A number of previous studies showed that NH_3 formation can be attributed primarily to the reaction of nitric oxide (NO) with hydrogen gas produced from the water–gas shift reaction between CO and water.[43,44] The hydrogen gas reduces NO to form NH_3 through multiple known and proposed pathways. Fuel-rich driving conditions are generally associated with more NO and CO supply and high temperature, which favor NH_3 formation. Most literature report high NH_3 emission ratios during fuel-rich driving conditions.[8,13−15,23]

To verify the representativeness of the individual car, we then measured 320 cars leaving the garage (flat surface, coasting to a stop sign). The measurement time, spatial coverage, and ambient temperature of this and the following measurements are listed in Table S1 (Supporting Information). The models of each vehicle driven by the sensor were recorded together with the point in time when each individual vehicle passed. The majority were midclass passenger cars with model years from 2000 to 2007. Honda (17%) and Toyota (16%) were the manufacturers with the largest number of vehicles. Because the measurements were performed during the evening rush hour of a winter day, most vehicles were near cold start conditions when passing the sensors. The average NH_3:CO emission ratio from the 320 cars in the garage is 0.019 ± 0.005 ppbv/ppbv, where the uncertainty is estimated from the measurement uncertainties of NH_3 and CO. This distribution is highly skewed, indicating a small number of high emitters and a majority of low emitters.

On-Road NH_3 Concentration Measurements. Three days of on-road NH_3 measurements were performed near Princeton, NJ on September 20 (drive #1), October 17 (drive #2), and November 11 (drive #3), 2012. CO was only measured in drive #3 due to sensor availability. The mean on-road NH_3:CO emission ratio was 0.029 ± 0.007 ppbv/ppbv in drive #3. The largest spatial and temporal coverage was performed in drive #2, covering a range of routes, including a six-lane urban highway with large traffic volumes (US Route 1, traffic volume ~10^5 vehicles/day), an urban–suburban road (County Route 533, traffic volume ~3×10^4 vehicles/day), and a suburban–rural road (County Route 614, traffic volume ~10^4 vehicles/day).[45]

The same routes on US Route 1 near Princeton were covered 3 times between 15:22 and 17:29 in drive #2, during which the traffic density continuously built up. Figure 2 illustrates the time evolution of NH_3 concentration distribution on US 1 toward the evening rush hour. The traffic density built up substantially during the second and third drive, and there were much more stop-and-go driving conditions. Our mean speed was only 43 km/h and 32 km/h in the last two drives, whereas the speed limit is 88.5 km/h. As the travel density built up, there were more acceleration events, which favor NH_3 generation in the TWC and contribute to the heavy tails toward higher NH_3 concentrations.

Figure 3 shows the correlations between NH_3 concentrations and traffic densities. The New Jersey Department of Transportation made hourly traffic counts during three consecutive days in 2009–2011 at nine locations along our driving route.[45] We segmented our driving routes in drive #2 according to their

dx.doi.org/10.1021/es4047704 | Environ. Sci. Technol. XXXX, XXX, XXX–XXX

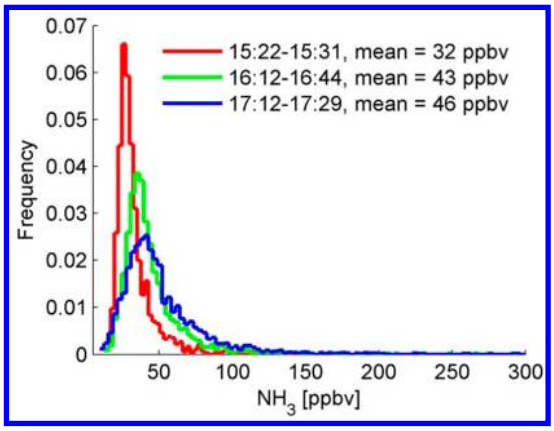

Figure 2. Time evolution of on-road NH_3 concentration distribution on US 1.

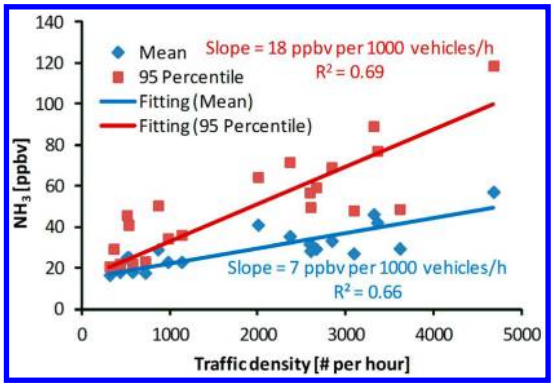

Figure 3. Correlations between mean and 95 percentile NH_3 concentrations measured on the segmented routes and traffic densities. The intercepts were forced to the regional background of 16 ppbv.

proximity to these traffic count locations. In many cases, we drove by traffic count locations multiple times. Detailed information on the driving time near each traffic count locations is listed in Table S2 in the Supporting Information. Significant positive correlations are found between the mean NH_3 concentrations on the segmented routes and traffic densities (correlations are significant at a level of 0.001). The mean NH_3 concentration increased by 7 ppbv per 1000 vehicles/h. Also shown in Figure 3 is the correlation between the 95 percentile of NH_3 concentrations on the segmented routes and traffic densities (correlations are significant at a level of 0.001). The 95 percentiles show a much larger slope (18 ppbv per 1000 vehicles/h), indicating that a relatively small percentage of the vehicle fleet emits a significant proportion of NH_3.

NH_3 Emission Factors and Driving Conditions. The mobile platform was fully equipped in California from January 21 to February 7, 2013, as part of the NASA DISCOVER-AQ campaign.[46] We covered 4300 km, including two major urban−suburban areas (San Francisco Bay area and Los Angeles Basin) and the suburban−rural areas in the San Joaquin valley. The total driving time was 81 h. In this section, we investigate the dependence of NH_3 emissions on road gradient on the freeways in the SF Bay area, where traffic speed was almost constant. We also investigate NH_3 emissions under a wide range of traffic speed in the Los Angeles Basin with no significant road gradient. The driving time and ambient conditions are summarized in Table S1(Supporting Information).

On-road measurements were performed on I-580 on February 3 and US Route 101 on February 4 and 5 in the SF Bay area. In all three cases, the mean wind velocity was light and varied by less than 1 m/s, such that we did not account for wind direction in our analyses. Both I-580 and US Route 101 have significant road gradients, often up to ±7% gradient (Figure S3−4, Supporting Information). Emission ratios are calculated using data measured on I-580 west bound in the East Bay area and on US 101 south bound in the North Bay area. Both routes are eight-lane freeways mainly in suburban areas (Supporting Information, Figure S5) and in free-flowing driving conditions. We drove at a constant speed in lane #3 (the central right lane) whenever it was possible. The driving speed was 92 ± 5 km/h, slightly lower than the speed limit, which ensured sampling the exhaust plumes produced by a variety of passing vehicles. The road gradient was derived by the instantaneous pressure gradient and GPS speed using the hydrostatic equation, with an uncertainty of 0.5% (eq 1 and associated text in the Supporting Information).

Emission ratios are calculated using NH_3, CO, and CO_2 concentrations, following the method introduced in the previous section. Figure 4 shows the dependence of NH_3:CO_2 and CO:CO_2 emission ratios on the road gradient. The emission ratio data are binned into 11 road gradient intervals, so that each bin has at least 60 s of net emission data. The 5, 25, 50, 75, and 95 percentiles of emission ratios within

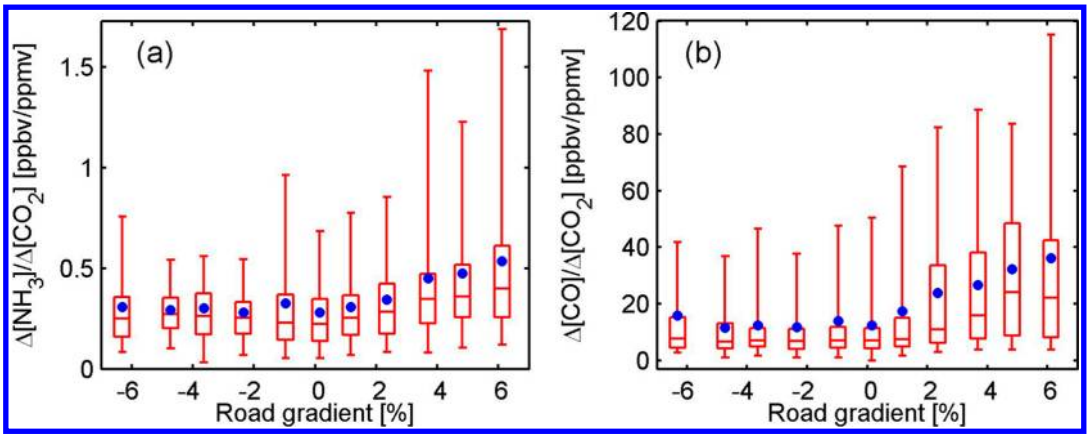

Figure 4. NH_3:CO_2 and CO:CO_2 emission ratios with road gradient. Five and 95 percentiles are denoted by whiskers of boxes, 25 and 75 percentiles are denoted by lower and upper boundaries of boxes, medians are denoted by central lines, and means are denoted by blue dots.

dx.doi.org/10.1021/es4047704 | Environ. Sci. Technol. XXXX, XXX, XXX−XXX

each bin are displayed as box-and-whisker plots, together with the arithmetic mean. Large variations of emission ratios were observed. Even for the same vehicle, emission factors can vary by 2 orders of magnitude due to driving conditions, as shown by dynamometer studies.[18] The variations among vehicles are also large, with skewed distributions, where the high emitters contribute to substantial fraction of total emissions.[21] In spite of the variability, both the mean NH_3:CO_2 (Figure 4a) and mean CO:CO_2 (Figure 4b) emission ratios showed significant enhancement when driving uphill. The variation of emission ratios was also higher. Tunnel studies have shown that driving uphill approximately doubled emission factors for CO compared to downhill, which generally agrees with our results.[30] As CO plays a key role in the water−gas shift reaction,[8] one should expect high NH_3 emissions as well.

The overall average NH_3:CO emission ratio is 0.031 ± 0.005 ppbv/ppbv, and it decreased with road gradient with an R^2 of 0.88 (Supporting Information, Figure S6). Although we have observed that for an individual car the NH_3:CO emission ratio increased with engine load in the garage measurements, the integrated on-road data show that CO emissions increased faster with road gradients and thus engine load than NH_3, which also agrees with roadside measurements.[20]

Although CO is a more sensitive tracer for vehicle emissions than CO_2, CO_2 is more important to quantify NH_3 emission factors, as CO_2 constitutes the majority of vehicular carbon emissions by mole fraction. The NH_3 EFs are expressed per kilogram of fuel burned using a carbon balance approach:

$$EF = \left(\frac{\Delta[NH_3]}{\Delta[CO_2] + \Delta[CO]}\right)\left(\frac{MW_{NH_3}}{MW_C}\right)w_C$$

Here MW_{NH3} and MW_C are the molecular weight of NH_3 and carbon. w_C = 0.85 is the mass fraction of carbon in gasoline. We neglect w_C of diesel (0.87) because diesel vehicles have been reported to have very limited contributions to on-road NH_3 emissions.[21]

Figure 5 shows the correlation between the average NH_3 EFs and the positive road gradients. Linear regression indicates that NH_3 EFs increase by 53 mg/kg when the road gradient increases by 1%, with an R^2 of 0.92. Emission factors measured by existing roadside and tunnel measurements in California are also plotted with the reported road gradient. The EFs measured in this study generally span the range reported by various studies, even though the literature measurements were conducted in diverse conditions. The high value in West LA (2008) is likely due to the strong acceleration at the measurement site, with an average of 0.85 m/s^2.[19] Higher NO_x emission ratios were also reported in West LA site than other on-road emission ratio studies.[28] On-road fleet variation may also contribute to the diversity of NH_3 EFs. Multiple roadside measurements have indicated that NH_3 EFs first increase and then decrease as a function of vehicle age, depending on two counteracting factors, catalyst reducing efficiency and NO (precursor of NH_3) emissions.[19−21]

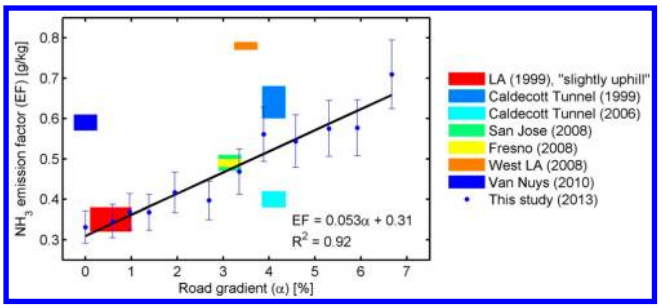

Figure 5. NH_3 EFs increase with road gradients. Error bars are estimated based on the measurement uncertainties. Color-coded rectangles denote existing EF measurements with reported road gradient. The vertical extension of each rectangle denotes the reported uncertainties. LA (1999) refers to Baum et al. (2001).[22] No quantitative road gradient was reported, but it should be within 1% according to Google Earth elevation data. Caldecott Tunnel (1999) refers to Kean et al.,[23] Caldecott Tunnel (2006) refers to Kean et al.,[24] San Jose, Fresno, and West LA (2008) refers to Bishop et al.,[19] and Van Nuys (2010) refers to Bishop et al.[20]

On January 27, 2013, we sampled NH_3 emission ratios in Los Angeles area. The driving route was mostly on flat terrain in the LA basin (Supporting Information, Figure S7). The total driving distance in the LA basin was 362 km, and driving time was 4.6 h. A wide range of driving speeds was sampled (Supporting Information, Figure S8). Zavala et al. classified their on-road measurements in Mexico City into stop-and-go, traffic, and cruise driving conditions, based on the speed of their mobile laboratory.[33] Their results indicated that CO EFs decreased from stop-and-go to cruise driving conditions, whereas NO EFs showed a weak increasing trend. In this study, we binned the NH_3 EF data according to the speed of mobile platform to get a more continuous relationship between EFs and traffic speed. The results are shown in Figure 6. The

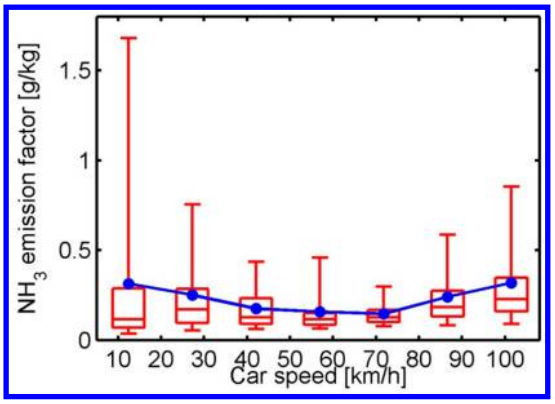

Figure 6. NH_3 EFs with driving speed in LA. The boxes and whiskers are defined as in Figure 4.

first two bins generally represent stop-and-go driving conditions, bins 2−5 represent in-traffic driving on the city roads, and bins 6−7 are freeway-driving. NH_3 EFs first decrease and then increase at highway speed. This dependence can be attributed to the emissions of two key precursors, CO and NO. According to existing vehicle emission inventory, EFs of CO and NO have shown a decreasing trend with speed but switch to an increasing trend at highway speed.[47]

In addition to the SF bay area and LA basin data, our measurements in three major cities (Fresno, Bakersfield, and Porterville) in the San Joaquin Valley were also added to include a wider range of driving conditions. Figure 7 shows the distribution of on-road NH_3 EFs measured in all the major urban areas covered during the DISCOVER-AQ campaign in California. Also shown in Figure 7 is the fit of a log−normal distribution. The EFs span about 4 orders of magnitude in range. The distribution of NH_3 EFs is almost symmetric at log scale (skewness = 0.045) but more peaked than a log−normal

dx.doi.org/10.1021/es4047704 | Environ. Sci. Technol. XXXX, XXX, XXX−XXX

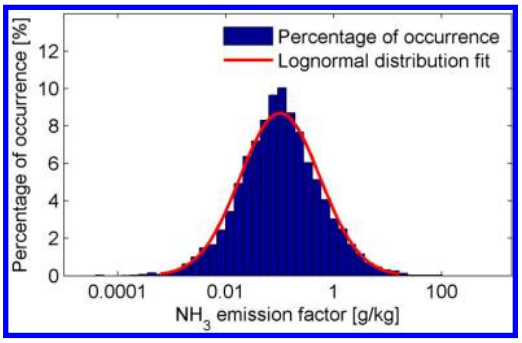

Figure 7. Distribution of on-road NH_3 EFs measured in all the major urban areas covered during the DISCOVER-AQ campaign in California. Red line shows the log−normal distribution fit with geometric mean of 0.37 g/kg and geometric standard deviation of 0.737.

distribution with a kurtosis of 3.5. The overall average of the EF data set is 0.49 g/kg, which generally falls within the range of the existing roadside measurements in California, as summarized in Figure 5.

CO was measured simultaneously in both New Jersey and California, and NH_3:CO emission ratios were used to assess on-road NH_3 sources. Nowak et al. used airborne gas/particulate NH_x and CO measurements to quantify NH_3 emissions from automobile sources in the South Coast Air Basin (SoCAB) during the CalNex 2010 experiment.[48] The mean NH_x:CO emission ratio reported downwind of the LA urban core was 0.033 ppbv/ppbv. The distributions of our NH_3:CO emission ratio measurements are shown as boxplots in Figure 8 together

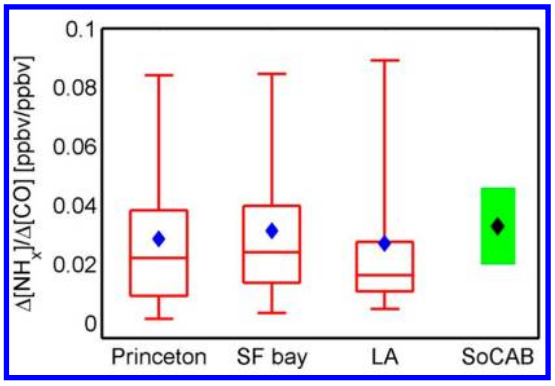

Figure 8. NH_3:CO emission ratio distributions in this study and NH_x:CO emission ratios measured by aircraft over South Coast Air Basin (SoCAB), CA in 2010.[48] The box-and-whisker plots are defined as in Figure 4. The vertical extension of the green rectangle denotes the reported ±1 standard deviation of the SoCAB measurements, and the black diamond denotes the mean value.

with the aircraft measurements over SoCAB. Because we measured in situ at the source location, we neglect the contributions of particulate phase ammonium. Our mean NH_3:CO emission ratio measured near San Francisco (0.031 ppbv/ppbv) and Los Angeles (0.027 ppbv/ppbv) is consistent with SoCAB NH_x:CO emission ratios. Although the climate and vehicle compositions are different, the on-road measurements near Princeton, NJ also showed similar NH_3:CO emission ratios (mean value = 0.029 ppbv/ppbv) compared to the California data.

IMPLICATIONS AND FUTURE DIRECTIONS

In 2011, the on-road NH_3 and CO emissions in New Jersey were estimated to be 2.4 Gg/yr and 0.48 Tg/yr, respectively, by the National Emission Inventory (NEI).[49] This gives an NH_3:CO emission ratio of 0.008 ppbv/ppbv, which is substantially smaller than our on-road measurements in New Jersey. The NEI also provides on-road NH_3 and CO emissions in California, which are 16 Gg/yr and 1.7 Tg/yr, respectively. This yields an NH_3:CO emission ratio of 0.018 ppbv/ppbv, also much smaller than our on-road measurements in California. As our on-road CO emission factor measurement also agrees well with recent tunnel measurements and emission models (Supporting Information, Figure S9), this implies that current on-road NH_3 emissions may be significantly underestimated and require further observational constraints. In situ validations of on-road NH_3 emission inventories are limited in the US, and most of them have been conducted in California (see Figure 5). However, few field measurements have been performed in the Northeast/Mid-Atlantic, where traffic and climate conditions are significantly different, and yet on-road emissions are substantial. This study sampled a representative fleet of cars in one specific area in the Northeast, but ultimately more measurements of larger spatial and temporal coverage will be needed.

We demonstrate for the first time in situ, mobile, open-path measurements of NH_3 emissions integrated across vehicles and locations in real-world conditions. Constant EFs based on dynamometer or roadside measurements have been used in NH_3 inventories over large area.[7,50,51] Nevertheless, on-road NH_3 emissions show significant spatial and temporal variations. The motivation of our measurements is to provide real-world observations of EFs over vast spatial coverage and wide range of fleet compositions. Our NH_3 EF measurements, combined with high resolution CO_2 emission inventories,[52−55] place a stronger constraint on current NH_3 emission inventories.

ASSOCIATED CONTENT

Supporting Information

Time scale of on-road emissions data, characterization of self emissions by the measurement vehicle, detailed roadside and on-road measurement information, additional information for on-road measurements in the SF bay area, and additional information for on-road measurements in the LA basin. This material is available free of charge via the Internet at http://pubs.acs.org.

AUTHOR INFORMATION

Corresponding Author

*E-mail: mzondlo@princeton.edu. Phone: 609-258-5037. Fax: 609-258-2799.

Present Address

[§]Now at Department of Physics and Engineering, Delaware State University, Dover, DE 19901

Notes

The authors declare no competing financial interest.

ACKNOWLEDGMENTS

The authors acknowledge people involved in the sensor development and deployment, including the research groups of Professors Elie Bou-Zeid, James Smith, and Claire Gmachl, as well as Minghui Diao, Josh DiGangi, and Anthony O'Brien at Princeton University. We thank the NASA DISCOVER-AQ

science team, especially James Crawford at NASA Langley Research Center and Trent Procter at USGS Forest Service. This research is supported by the Center for Mid-Infrared Technologies for Health and the Environment (MIRTHE) under National Science Foundation Grant No. EEC-0540832. Kang Sun gratefully acknowledges support by a NASA Earth and Space Science Fellowship (NN12AN64H).

REFERENCES

(1) IPCC. *Intergovernmental Panel on Climate Change*; Cambridge University Press: Cambridge, U.K., 2007.

(2) Pinder, R. W.; Gilliland, A. B.; Dennis, R. L. Environmental impact of atmospheric NH_3 emissions under present and future conditions in the eastern United States. *Geophys. Res. Lett.* **2008**, DOI: 10.1029/2008GL033732.

(3) Clarisse, L.; Clerbaux, C.; Dentener, F.; Hurtmans, D.; Coheur, P. F. Global ammonia distribution derived from infrared satellite observations. *Nat. Geosci.* **2009**, *2* (7), 479−483.

(4) Shephard, M. W.; Cady-Pereira, K. E.; Luo, M.; Henze, D. K.; Pinder, R. W.; Walker, J. T.; Rinsland, C. P.; Bash, J. O.; Zhu, L.; Payne, V. H.; Clarisse, L. TES ammonia retrieval strategy and global observations of the spatial and seasonal variability of ammonia. *Atmos. Chem. Phys.* **2011**, *11* (20), 10743−10763.

(5) Walker, J. M.; Philip, S.; Martin, R. V.; Seinfeld, J. H. Simulation of nitrate, sulfate, and ammonium aerosols over the United States. *Atmos. Chem. Phys.* **2012**, *12* (22), 11213−11227.

(6) EDGAR v4.2 Ammonia inventory. http://edgar.jrc.ec.europa.eu/overview.php?v=42#. (accessed December 2012).

(7) Bouwman, A. F.; Lee, D. S.; Asman, W. A. H.; Dentener, F. J.; Van Der Hoek, K. W.; Olivier, J. G. J. A global high-resolution emission inventory for ammonia. *Global Biogeochem. Cycles* **1997**, *11* (4), 561−587.

(8) Livingston, C.; Rieger, P.; Winer, A. Ammonia emissions from a representative in-use fleet of light and medium-duty vehicles in the California South Coast Air Basin. *Atmos. Environ.* **2009**, *43* (21), 3326−3333.

(9) Li, Y. Q.; Schwab, J. J.; Demerjian, K. L. Measurements of ambient ammonia using a tunable diode laser absorption spectrometer: Characteristics of ambient ammonia emissions in an urban area of New York City. *J. Geophys. Res.: Atmos.* **2006**, DOI: 10.1029/2005JD006275.

(10) Meng, Z. Y.; Lin, W. L.; Jiang, X. M.; Yan, P.; Wang, Y.; Zhang, Y. M.; Jia, X. F.; Yu, X. L. Characteristics of atmospheric ammonia over Beijing, China. *Atmos. Chem. Phys.* **2011**, *11* (12), 6139−6151.

(11) Gong, L.; Lewicki, R.; Griffin, R. J.; Flynn, J. H.; Lefer, B. L.; Tittel, F. K. Atmospheric ammonia measurements in Houston, TX using an external-cavity quantum cascade laser-based sensor. *Atmos. Chem. Phys.* **2011**, *11* (18), 9721−9733.

(12) Parrish, D. D.; Zhu, T. Clean air for megacities. *Science* **2009**, *326* (5953), 674−675.

(13) Bielaczyc, P.; Szczotka, A.; Swiatek, A.; Woodburn, J. *Investigations of Ammonia Emissions from Euro 5 Passenger Cars Over a Legislative Driving Cycle*. Proceedings of the FISITA 2012 World Automotive Congress; Springer-Verlag: Berlin, 2012; pp 671−685.

(14) Bielaczyc, P.; Szczotka, A.; Swiatek, A.; Woodburn, J. A comparison of ammonia emission factors from light-duty vehicles operating on gasoline, liquefied petroleum gas (LPG) and compressed natural gas (CNG). *SAE Int. J. Fuels Lubr.* **2012**, *5* (2), 751−759.

(15) Huai, T.; Durbin, T. D.; Miller, J. W.; Pisano, J. T.; Sauer, C. G.; Rhee, S. H.; Norbeck, J. M. Investigation of NH3 emissions from new technology vehicles as a function of vehicle operating conditions. *Environ. Sci. Technol.* **2003**, *37* (21), 4841−4847.

(16) Huai, T.; Durbin, T. D.; Rhee, S. H.; Norbeck, J. M. Investigation of emission rates of ammonia, nitrous oxide and other exhaust compounds from alternative fuel vehicles using a chassis dynamometer. *Int. J. Automot. Technol.* **2003**, *4* (1), 9−19.

(17) Huai, T.; Durbin, T. D.; Younglove, T.; Scora, G.; Barth, M.; Norbeck, J. M. Vehicle specific power approach to estimating on-road NH_3 emissions from light-duty vehicles. *Environ. Sci. Technol.* **2005**, *39* (24), 9595−9600.

(18) Heeb, N. V.; Forss, A.-M.; Brühlmann, S.; Lüscher, R.; Saxer, C. J.; Hug, P. Three-way catalyst-induced formation of ammonia—velocity- and acceleration-dependent emission factors. *Atmos. Environ.* **2006**, *40* (31), 5986−5997.

(19) Bishop, G. A.; Peddle, A. M.; Stedman, D. H.; Zhan, T. On-road emission measurements of reactive nitrogen compounds from three california cities. *Environ. Sci. Technol.* **2010**, *44* (9), 3616−3620.

(20) Bishop, G. A.; Schuchmann, B. G.; Stedman, D. H.; Lawson, D. R. Multispecies remote sensing measurements of vehicle emissions on Sherman Way in Van Nuys, California. *J. Air Waste Manage. Assoc.* **2012**, *62* (10), 1127−1133.

(21) Burgard, D. A.; Bishop, G. A.; Stedman, D. H. Remote sensing of ammonia and sulfur dioxide from on-road light duty vehicles. *Environ. Sci. Technol.* **2006**, *40* (22), 7018−7022.

(22) Baum, M. M.; Kiyomiya, E. S.; Kumar, S.; Lappas, A. M.; Kapinus, V. A.; Lord, H. C., III Multicomponent remote sensing of vehicle exhaust by dispersive absorption spectroscopy. 2. Direct on-road ammonia measurements. *Environ. Sci. Technol.* **2001**, *35* (18), 3735−3741.

(23) Kean, A. J.; Harley, R. A.; Littlejohn, D.; Kendall, G. R. On-road measurement of ammonia and other motor vehicle exhaust emissions. *Environ. Sci. Technol.* **2000**, *34* (17), 3535−3539.

(24) Kean, A. J.; Littlejohn, D.; Ban-Weiss, G. A.; Harley, R. A.; Kirchstetter, T. W.; Lunden, M. M. Trends in on-road vehicle emissions of ammonia. *Atmos. Environ.* **2009**, *43* (8), 1565−1570.

(25) von Bobrutzki, K.; Braban, C. F.; Famulari, D.; Jones, S. K.; Blackall, T.; Smith, T. E. L.; Blom, M.; Coe, H.; Gallagher, M.; Ghalaieny, M.; McGillen, M. R.; Percival, C. J.; Whitehead, J. D.; Ellis, R.; Murphy, J.; Mohacsi, A.; Pogany, A.; Junninen, H.; Rantanen, S.; Sutton, M. A.; Nemitz, E. Field inter-comparison of eleven atmospheric ammonia measurement techniques. *Atmos. Meas. Tech.* **2010**, *3* (1), 91−112.

(26) Pierson, W. R.; Brachaczek, W. W. Emissions of ammonia and amines from vehicles on the road. *Environ. Sci. Technol.* **1983**, *17* (12), 757−760.

(27) Franco, V.; Kousoulidou, M.; Muntean, M.; Ntziachristos, L.; Hausberger, S.; Dilara, P. Road vehicle emission factors development: A review. *Atmos. Environ.* **2013**, *70*, 84−97.

(28) Hudda, N.; Fruin, S.; Delfino, R.; Sioutas, C. Efficient determination of vehicle emission factors by fuel use category using on-road measurements: Downward trends on Los Angeles freight corridor I-710. *Atmos. Chem. Phys.* **2013**, *13*, 347−357.

(29) Cicero-Fernández, P.; Long, J. R.; Winer, A. M. Effects of grades and other loads on on-road emissions of hydrocarbons and carbon monoxide. *J. Air Waste Manage. Assoc.* **1997**, *47* (8), 898−904.

(30) Kean, A. J.; Harley, R. A.; Kendall, G. R. Effects of vehicle speed and engine load on motor vehicle emissions. *Environ. Sci. Technol.* **2003**, *37* (17), 3739−3746.

(31) Lee, T.; Frey, H. C. Evaluation of representativeness of site-specific fuel-based vehicle emission factors for route average emissions. *Environ. Sci. Technol.* **2012**, *46* (12), 6867−6873.

(32) Herndon, S. C.; Jayne, J. T.; Zahniser, M. S.; Worsnop, D. R.; Knighton, B.; Alwine, E.; Lamb, B. K.; Zavala, M.; Nelson, D. D.; McManus, J. B.; Shorter, J. H.; Canagaratna, M. R.; Onasch, T. B.; Kolb, C. E. Characterization of urban pollutant emission fluxes and ambient concentration distributions using a mobile laboratory with rapid response instrumentation. *Faraday Discuss.* **2005**, *130* (0), 327−339.

(33) Zavala, M.; Herndon, S.; Wood, E.; Onasch, T.; Knighton, W.; Marr, L.; Kolb, C.; Molina, L. Evaluation of mobile emissions contributions to Mexico City's emissions inventory using on-road and cross-road emission measurements and ambient data. *Atmos. Chem. Phys.* **2009**, *9*, 6305−6317.

(34) McDermitt, D.; Burba, G.; Xu, L.; Anderson, T.; Komissarov, A.; Riensche, B.; Schedlbauer, J.; Starr, G.; Zona, D.; Oechel, W. A new low-power, open-path instrument for measuring methane flux by eddy covariance. *Appl. Phys. B: Lasers Opt.* **2011**, *102* (2), 391−405.

(35) Zondlo, M. A.; Paige, M. E.; Massick, S. M.; Silver, J. A. Vertical cavity laser hygrometer for the National Science Foundation Gulfstream-V aircraft. *J. Geophys. Res.: Atmos.* **2010**, DOI: 10.1029/2010JD014445.
(36) Khan, A.; Schaefer, D.; Tao, L.; Miller, D. J.; Sun, K.; Zondlo, M. A.; Harrison, W. A.; Roscoe, B.; Lary, D. J. Low Power Greenhouse Gas Sensors for Unmanned Aerial Vehicles. *Remote Sens.* **2012**, *4* (5), 1355−1368.
(37) Tao, L.; Sun, K.; Khan, M. A.; Miller, D. J.; Zondlo, M. A. Compact and portable open-path sensor for simultaneous measurements of atmospheric N_2O and CO using a quantum cascade laser. *Opt. Express* **2012**, *20* (27), 28106−28118.
(38) Miller, D. J.; Sun, K.; Tao, L.; Khan, M. A.; Zondlo, M. A. Open-path, quantum cascade-laser-based sensor for high-resolution atmospheric ammonia measurements. *Atmos. Meas. Tech.* **2014**, *7* (1), 81−93.
(39) Dharamsi, A. N.; Bullock, A. M. Applications of wavelength-modulation spectroscopy in resolution of pressure and modulation broadened spectra. *Appl. Phys. B* **1996**, *63* (3), 283−292.
(40) Sun, K.; Tao, L.; Miller, D.; Khan, M. A.; Zondlo, M. Inline multi-harmonic calibration method for open-path atmospheric ammonia measurements. *Appl. Phys. B: Lasers Opt.* **2013**, *110* (2), 213−222.
(41) Xu, L.; Penner, J. Global simulations of nitrate and ammonium aerosols and their radiative effects. *Atmos. Chem. Phys.* **2012**, *12* (20), 9479−9504.
(42) Jimenez, J.; McManus, J.; Shorter, J.; Nelson, D.; Zahniser, M.; Koplow, M.; McRae, G.; Kolb, C. Cross road and mobile tunable infrared laser measurements of nitrous oxide emissions from motor vehicles. *Chemosphere: Global Change Sci.* **2000**, *2* (3), 397−412.
(43) Shelef, M.; Gandhi, H. S. Ammonia Formation in the Catalytic Reduction of Nitric Oxide. III. The Role of Water Gas Shift, Reduction by Hydrocarbons, and Steam Reforming. *Product R&D* **1974**, *13* (1), 80−85.
(44) Gandhi, H. S.; Shelef, M. Effects of sulphur on noble metal automotive catalysts. *Appl. Catal.* **1991**, *77* (2), 175−186.
(45) New Jersey Roadway Information and Traffic Monitoring System Program. http://www.state.nj.us/transportation/refdata/roadway/traffic.shtm. (accessed January 2013).
(46) DISCOVER-AQ | NASA. http://www.nasa.gov/mission_pages/discover-aq/#.UrNqtfRDvi0 (accessed December 2013).
(47) California Department of Transportation. http://www.dot.ca.gov/hq/env/air/pages/emfac.htm (accessed August 2013).
(48) Nowak, J. B.; Neuman, J. A.; Bahreini, R.; Middlebrook, A. M.; Holloway, J. S.; McKeen, S. A.; Parrish, D. D.; Ryerson, T. B.; Trainer, M. Ammonia sources in the California South Coast Air Basin and their impact on ammonium nitrate formation. *Geophys. Res. Lett.* **2012**, DOI: 10.1029/2012GL051197.
(49) NEI The National Emission Inventory 2011. http://www.epa.gov/ttnchie1/net/2011inventory.html (accessed December 2013).
(50) Huang, X.; Song, Y.; Li, M.; Li, J.; Huo, Q.; Cai, X.; Zhu, T.; Hu, M.; Zhang, H. A high-resolution ammonia emission inventory in China. *Global Biogeochem. Cycles* **2012**, *26* (1).
(51) Zheng, J.; Yin, S.; Kang, D.; Che, W.; Zhong, L. Development and uncertainty analysis of a high-resolution NH_3 emissions inventory and its implications with precipitation over the Pearl River Delta region, China. *Atmos. Chem. Phys.* **2012**, *12*, 7041−7058.
(52) Brondfield, M. N.; Hutyra, L. R.; Gately, C. K.; Raciti, S. M.; Peterson, S. A. Modeling and validation of on-road CO_2 emissions inventories at the urban regional scale. *Environ. Pollut.* **2012**, *170*, 113−123.
(53) Gately, C. K.; Hutyra, L.; Wing, I.; Brondfield, M. A bottom up approach to on-road CO_2 emissions estimates: improved spatial accuracy and applications for regional planning. *Environ. Sci. Technol.* **2013**, *47* (5), 2423−2430.
(54) Gurney, K. R.; Razlivanov, I.; Song, Y.; Zhou, Y.; Benes, B.; Abdul-Massih, M. Quantification of fossil fuel CO_2 emissions on the building/street scale for a large US City. *Environ. Sci. Technol.* **2012**, *46* (21), 12194−12202.
(55) Gurney, K. R.; Mendoza, D. L.; Zhou, Y.; Fischer, M. L.; Miller, C. C.; Geethakumar, S.; de la Rue du Can, S. High resolution fossil fuel combustion CO_2 emission fluxes for the United States. *Environ. Sci. Technol.* **2009**, *43* (14), 5535−5541.